

Monte Carlo simulations of highly anisotropic two-dimensional hard dumbbell-shaped molecules: Nonperiodic phase between fluid and dense solid

K. W. Wojciechowski

Institute of Molecular Physics, Polish Academy of Sciences, Smoluchowskiego 17/19, 60-179 Poznań, Poland and International Centre for Theoretical Physics, Trieste, Italy*

(Received 15 April 1991; revised manuscript received 28 January 1992)

Monte Carlo simulations of a two-dimensional hard homonuclear dumbbell-shaped-molecules system with a high anisotropy parameter $d^* = 0.924$ were performed for three different thermodynamic states: (i) fluid; (ii) aperiodic molecular solid, whose molecular arrangements can be represented by certain decorations of the *kagomé* lattice; and (iii) high-density solid, whose molecular structure corresponds to dense packing of the dumbbell-shaped molecules. The latter structure was exemplified in this study by a herring-bone-type crystal. Explicit calculations of the free energies of the different states, together with the analysis of the melting region, show that the aperiodic solid structures form a thermodynamically stable phase between the fluid and the dense solid. The equation of state, structural properties, and the locations of the phase transitions are reported. The role of the degeneracy entropy in the aperiodic phase is discussed.

I. INTRODUCTION

Hard-body systems, despite their simplicity, can reproduce many essential features and behaviors of real systems.¹⁻⁶ There is no doubt that the molecular shape is important in determining physical properties of molecular systems and, in particular, their phase diagrams. However, the phase diagrams are well established only for a few shapes.^{2,3,6-19} There exists a basic hard-body shape for which the phase diagram has not yet been determined quantitatively, although some qualitative results have been obtained.²⁰ This is the case of the hard homonuclear dumbbell, the crudest model for a diatomic molecule and the simplest nonconvex body.²¹ The hard homonuclear dumbbell consists of two fused hard spheres, "atoms," of diameter σ and centers at a distance $d = d^*\sigma$ (where d^* is the anisotropy parameter). One of the reasons for having interest in the properties of a system of such molecules is the strong degeneracy of its close-packed structure at $d^* = 1$. Strong degeneracy of low-energy states is characteristic for disordered systems such as glasses²² and spin glasses,²³ which are the subject of current interest in physics. When the degeneracy leads to a positive entropy per particle, this entropy can play a crucial role in determining the properties of the system. In some cases this leads to striking behaviors as, e.g., for certain quasicrystalline materials²⁴ in which the aperiodic (quasicrystalline) phase is stabilized by this entropy.²⁵ As it will be shown below, in the case of dumbbells (at d^* close to unity) the degeneracy entropy also stabilizes certain molecular aperiodic phase. This aperiodic phase can be thought of as an "atomic crystal," and the structural transitions between it and a crystalline phase can be considered as the simplest example of a phase transition between atomic and molecular crystal.²⁰

In the present work the two-dimensional (2D) version of the system of hard homonuclear dumbbells is con-

sidered. Each molecule (hereafter referred to as the *dumbbell*, for the sake of brevity) consists of two equidiameter hard discs of centers at the distance $d^*\sigma$; the system is hereafter referred to as the HHD system. We report the equation of state (EOS) and structural properties of the system that were obtained by the Monte Carlo (MC) simulations at a single value of the anisotropy parameter, chosen close to 1. An estimate of the stability range of the aperiodic phase with respect to d^* is given. The whole phase diagram of the system for $0 \leq d^* \leq 1$ will be described elsewhere.²⁶

There are a few reasons to justify studies of the 2D systems. (i) The model is conceptually simpler than its three-dimensional (3D) counterpart, and the possibility of direct observations of the molecular structures is useful for their analysis. (ii) A much narrower hysteresis loop is expected at the melting transition of the 2D system if compared to its 3D version. [This is done *by analogy* to the 2D hard disks for which the globally densest triangular structure is at the same time the densest locally. (Such a property does not hold for 3D hard spheres for which the tetrahedron is the densest cluster; no complete filling of the space by the tetrahedrons exists.) Hence, no competition between the triangular lattice and any other (locally denser) "glassy" structure is expected at freezing. It is then natural to expect that at $d^* = 1$ the system should easily freeze into the triangular lattice of the disk "atoms" constituting *dimers* (at $d^* = 1$, the molecules will be called dimers). A small decrease of d^* should not change this situation greatly.] A narrow hysteresis loop in a small system constitutes relatively accurate bracketing of the melting transition region. Moreover, there exist simple, efficient, and accurate methods for computing the free energy in model systems,²⁷ and these methods can be easily applied to the dumbbells. Such a situation not only allows for cross-checking the consistency of the obtained results but demonstrates in a convincing way

that the system studied does not freeze into a periodic crystalline structure. (iii) Experiments have been done with monolayers of diatomics adsorbed on crystalline surfaces.²⁸ In the simplest approximation these monolayers can be considered as 2D systems and the HHD system can be thought of as a crude model for them. (iv) The system is interesting from a purely theoretical point of view, providing information on the phase diagram of a low-dimensional model of anisotropic particles. Finally, (v) lower dimension also means a lower number of the degrees of freedom in the system, which should result in reduction of computer time.

The organization of the paper is as follows: In the next section (II) some preliminary information concerning the system studied is given; in Sec. III the simulation results of the EOS and structural properties of the system are described; in Sec. IV free-energy calculations and phase-transition locations are discussed; and in Sec. V some remarks concerning the degeneracy entropy and the phase transitions in the system are presented. The last section (VI) contains the summary of results.

II. PRELIMINARIES

Heuristic reasoning and free-volume arguments suggest the existence of a few phases in the HHD system, depending on the anisotropy parameter and the density values.²⁰ In particular, in the *dimer* system, $d^*=1$, the thermodynamic stability of a certain solid, with the dimers distributed aperiodically, was suggested for the whole density range of the solid.^{18,20} Stability of the aperiodic phase, which was expected to have its source in the strong degeneracy of the close-packed structure of the dimers²⁰ was recently confirmed by computer simulations.¹⁹ The configurational degeneracy of the dimer close-packed structures leads to a *positive* entropy per particle, $s_{DC} \approx 0.857k_B T$.²⁹ The orientations of the dimers and the positions of their centers of mass in the aperiodic phase are not quite random: the disk atoms form a triangular lattice, perfect at close packing and slightly disturbed at lower densities of the solid. This indicates that the dimer arrangements in the aperiodic structure are related to certain decorations of the *kagomé* lattice by the dimer centers of mass. As it is easy to check, the rule for constructing these decorations requires that in each unit hexagon of the *kagomé* lattice exactly one site is occupied by the center of mass of a dimer.²⁰ Among such configurations there exist countably many regular (*periodic* or *nonperiodic self-similar*) decorations. Probability of a random choice of any regular decoration is, however, zero as the number of all the decorations is uncountably. Hence, there are uncountably many *irregular* decorations (which are neither periodic nor self-similar). Such decorations of the *kagomé* lattice will be further referred to as *ideal random decorations* (IRD's). Aperiodic molecular structures obtained from the IRD's, by allowing the molecules to move, represent the so-called *disordered* (or *degenerate*) *crystal* (DC).^{19,20}

When $d^* = 1 - \epsilon$ ($\epsilon > 0$) the DC structure, see Fig. 1(a), into which the HHD fluid should freeze when ϵ is

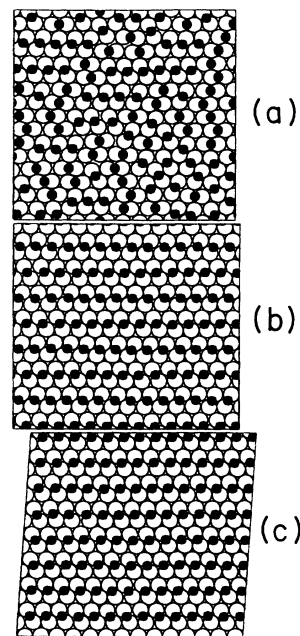


FIG. 1. Examples of solid structures of the dumbbells at $d^*=0.924$: (a) DC structure, (b) HB crystal, and (c) simple oblique-lattice crystal.

small,²⁰ cannot be stable in the whole density range of the solid. The symmetry of the *kagomé* lattice must be broken at high densities, and the system should change its structure. This is so because certain crystalline structures offer denser packings of the dumbbells, $d^* < 1$, than the structure obtained by the random decoration of the *kagomé* lattice (see Fig. 2), even if some distortions are allowed. The *kagomé* lattice is only a convenient idealization which generates the DC structures of the dumbbells. Except at close packing of the dimers, the observed probability density maxima of the orientations and positions of the dumbbells show some (local) deviations from the IRD. This is easy to understand taking into account that below the close-packing limit the interparticle interactions do not have the *kagomé* lattice symmetry. It is worth noting that, except at $d^*=1$, the IRD much

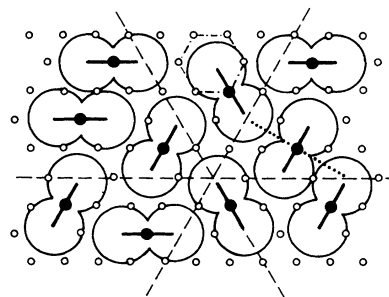


FIG. 2. Example of the IRD for dumbbells at $d^*=0.924$. The dashed lines correspond to the axes of the conjugated triangular lattice, the thin dash-dotted line marks a unit hexagon of the *kagomé* lattice, and the dotted line indicates the "short" molecular axis of one of the dumbbells.

overestimates the area per particle obtained for the real random close-packed structures (see Sec. III). The reason is clear from Fig. 2; only a part of the dumbbells are in contact at the densest IRD. The experimentally estimated density of the real random packing of the dumbbells at a certain ϵ is marked by an asterisk in Fig. 3. One of the simplest crystalline packings that is denser than the randomly decorated *kagomé* lattice is the herring-bone-pattern (HB) crystal; see Fig. 1(b). No packing of the dumbbells is known that reaches higher density in the thermodynamic limit than that of the close-packed HB crystal.³⁰ Hence, in the following the HB crystal is assumed to be the densest structure of the dumbbells. Its area per particle at close packing is

$$v_{\text{HB}}(d^*) \equiv v_{\text{cp}}(d^*) = [\sqrt{3}/2 + d^*(1 - d^{*2}/4)^{1/2}] \sigma^2. \quad (1)$$

For comparison, the minimal area per particle of the IRD can be expressed as

$$v_{\text{DC}}(d^*) = \sqrt{3} [d^*/2 + (1 - 3d^{*2}/4)^{1/2}]^2 \sigma^2. \quad (2)$$

Both these quantities are plotted in Fig. 3. As it can be seen, $v_{\text{HB}} \leq v_{\text{DC}}$; the equality holds only at $d^* = 1$.

There exist infinitely many packings of the dumbbells ($\epsilon > 0$), mostly aperiodic, with the density, $\rho_{\text{cp}} \equiv 1/v_{\text{cp}}$, equal to that of the close-packed HB crystal. Some of them can be obtained by changing orientations of consecutive molecular rows in the HB structure [the simplest example³¹ is shown in Fig. 1(c)]. It can be seen in Fig. 4(b) that these structures do not exhaust all the possibilities. A question arises whether the degeneracy entropy per particle of the highest-density state is zero or positive, as in the case of the DC structures. A rigorous answer to this question is not known at present. However, analysis of a certain lattice model shown in Fig. 4 and described in Appendix A suggests that this entropy is zero. Thus, it is assumed further that the degeneracy entropy per particle of the “ground state” of the HHD system ($\epsilon > 0$) is zero. If this assumption were not true, i.e., if the degeneracy entropy of dumbbells at close packing were small but *positive*, then the HHD system would not form any “standard” crystalline phase at $d^* > 0$. Its stable phase at the highest densities would then be in

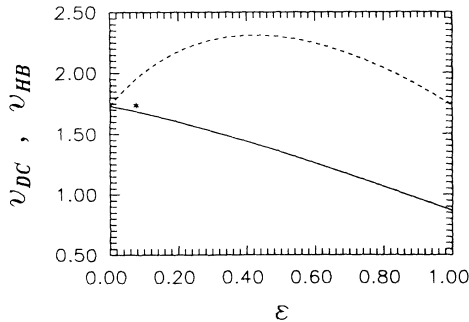


FIG. 3. Area per particle at the closest packing of the dumbbell-shaped molecules as a function of $\epsilon = 1 - d^*$: (i) IRD (dotted line) and (ii) HB crystal (continuous line). The star at $\epsilon = 0.076$ represents an MC estimate of the close-packing limit of real random structures of the dumbbells.

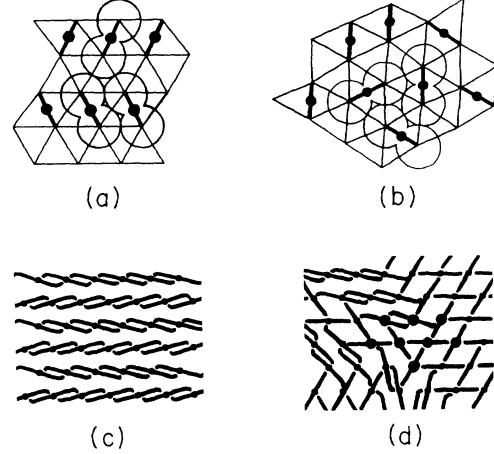


FIG. 4. Triangular tilings of the plane corresponding to (a) the HB crystal, and (b) an aperiodic packing of the same density. Two kinds of triangles are used: (i) the isosceles triangle, whose base (shorter side) is equal to $d = d^* \sigma$ and the other sides are equal to σ , and (ii) the equilateral triangle of the side σ . It is easy to check that given a tiling at certain d^* then one can construct a tiling at a different anisotropy parameter d_1^* , changing the lengths of the bases of all the isosceles triangles from d to $d_1 = d_1^* \sigma$. This property can be used to map the tiling problem onto a certain lattice model, namely, in the limit of zero length of the short sides of the isosceles triangles (the sides of the equilateral triangles remain intact) one obtains a lattice model being a certain decoration, see text, of the triangular lattice by trimers. (In this limit the long axes of the rhombi formed by pairs of isosceles triangles are transformed into pairs of parallel, neighboring bonds, forming trimers. The latter are represented either by straight-line segments or by tilde marks and their mirror images for reasons specified in Appendix A.) The decoration (c) corresponds to the HB crystal whereas a part (larger dots) of (d) corresponds to the aperiodic packing shown in (b).

many aspects similar to the DC phase of the dimers. This would have only minor influence on the quantitative analysis presented in this work and would result in a slight lowering of the pressure of the structural transition between the DC phase and the high-density phase.

The above discussion suggests the following picture for the equation of state (EOS) of the HHD system at $\epsilon \rightarrow 0^+$: (i) At low densities the system is fluid (there is no gas-liquid condensation transition in the system because no attractive forces are present), (ii) at a certain density the fluid freezes into the DC phase which, at even higher density, transforms into (iii) a high-density solid phase of the highest packing rate. The later phase is exemplified here by the HB crystalline structure. Some consequences of this choice will be discussed in Sec. VI. In this paper we take $\epsilon = 0.076$, which leads to $d^* = 0.924$, a value slightly above the minimal value of the anisotropy parameter for which the DC phase is stable in the free-volume approximation.²⁰

At the end of this section we would like to note that the well-known problem of the long-range translation order in the 2D solids³² has not been taken into account in this work. This is (i) to avoid unnecessary complications

and (ii) because the structures considered and the transitions between them are believed to have their source in the local molecular arrangements. Thus, a local treatment should be sufficient to describe them.

III. THE EQUATION OF STATE AND THE STRUCTURE DETERMINATION

The EOS and the structural properties of the system were determined by using the MC method in the NpT ensemble.^{33-35,8,3(b)}

The fluid was simulated in a square box. In the subsequent runs the pressure was increased from its minimal value $p^* \equiv p\sigma^2/k_B T = 0.2$ up to $p^* = 11.5$, where the system froze into a certain DC structure with some defects frozen in.

For the solid structures the box shape was allowed to fluctuate freely.³⁶ This eliminates internal stresses that would accompany any misfit between the box shape and the unit-cell parameters. The simulations of the HB crystal were started at the highest pressure $p^* = 60$. Then, in the following runs, the pressure was decreased until the system melted at $p^* = 8.5$. The simulations of the DC state were initiated at $p^* = 12$; the starting configuration was a certain IRD generated at $v^* \equiv v/v_{cp} = 1.18$, where v is the area per dumbbell. The pressure was increased up to $p^* = 50$ and then decreased down to melting, which has occurred at $p^* = 10$.

In the DC state some collective moves of certain molecular clusters were also introduced in order to sample different molecular arrangements in this phase. This was done because, in the absence of such collective moves, the solid was observed to preserve its molecular arrangement down to melting. The idea of the collective moves is presented in Fig. 5 (details are described in Appendix B). It is worth noting that such collective moves combined with the standard molecular moves are, in principle, sufficient for ergodicity in the DC state in the thermodynamic limit. This is because (i) there exists no IRD in which none of the clusters shown in Figs. 5 (or their rotation images) is contained³⁷ and because (ii) using the above collective moves one can transform any IRD (generating a certain real DC structure) into a decoration with all dumbbells parallel. The proof, which is not complicated but rather lengthy, consists of two parts. First, one shows that by applying these moves to any IRD it is possible to construct an infinite row of neighboring mole-

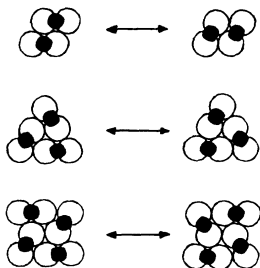


FIG. 5. Idea of the collective moves of the molecular clusters discussed in the text.

cules with long axes parallel to the direction of the line containing their centers. Second, starting from this row one constructs, by applying the collective moves, a stripe of arbitrary number of such rows. For a finite width of the stripe, the arrangement of the molecules in such a stripe is either equivalent to a perfect oblique lattice of the molecules or to the oblique lattice with one stacking fault. When the width tends to infinity, the difference between these two cases can be neglected because the stacking fault can be removed to infinity. Even these collective moves were found to be not efficient at high densities, and above the dimensionless pressure $p^* = 30$ the system remained trapped into a single structure.

The simulations were performed for a system of $N = 112$ molecules and the averages were calculated for $(2-4) \times 10^4$ trial steps per molecule (cycles) after $(0.5-2) \times 10^4$ cycles equilibration. Some test runs performed for $N = 448$ dumbbells did not reveal any number dependence exceeding the experimental error. A series of runs has also been performed for $N = 960$ in the NpT ensemble near melting to analyze the structural properties of the system (these runs are discussed in the Sec. V). The molecular moves consisted of translations of the molecular centers accompanied by simultaneous rotations of the molecular axes. The maximal orientational displacement allowed (in radians) was $(2/d^*)$ times larger

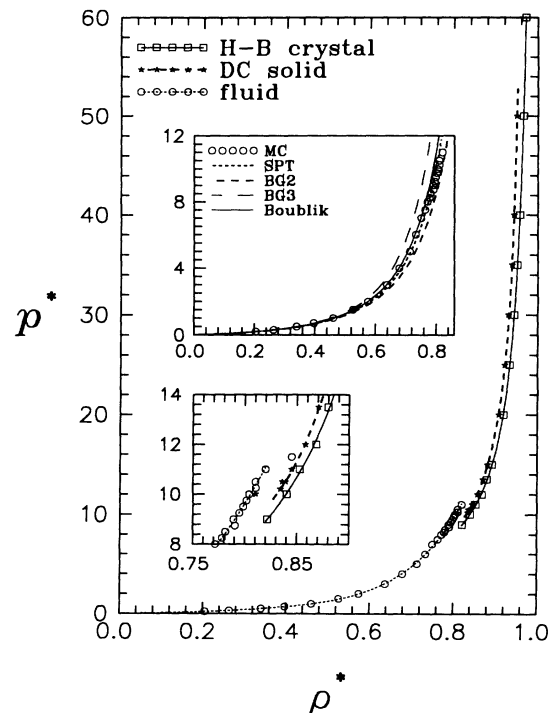


FIG. 6. EOS for the different phases of the dumbbells at $d^* = 0.924$. The lines in the main figure are drawn to guide the eyes. The upper inset presents some theoretical approximations for the fluid: (a) the semiempirical Boublik's equation, Eq. (5) in Ref. 38, continuous line; (b) the scaled particle theory result, Eq. (3) in Ref. 38, dotted line; (c) the second-order γ expansion, and (d) the third-order γ expansion (dashed lines). The lower inset contains an enlargement of the melting region.

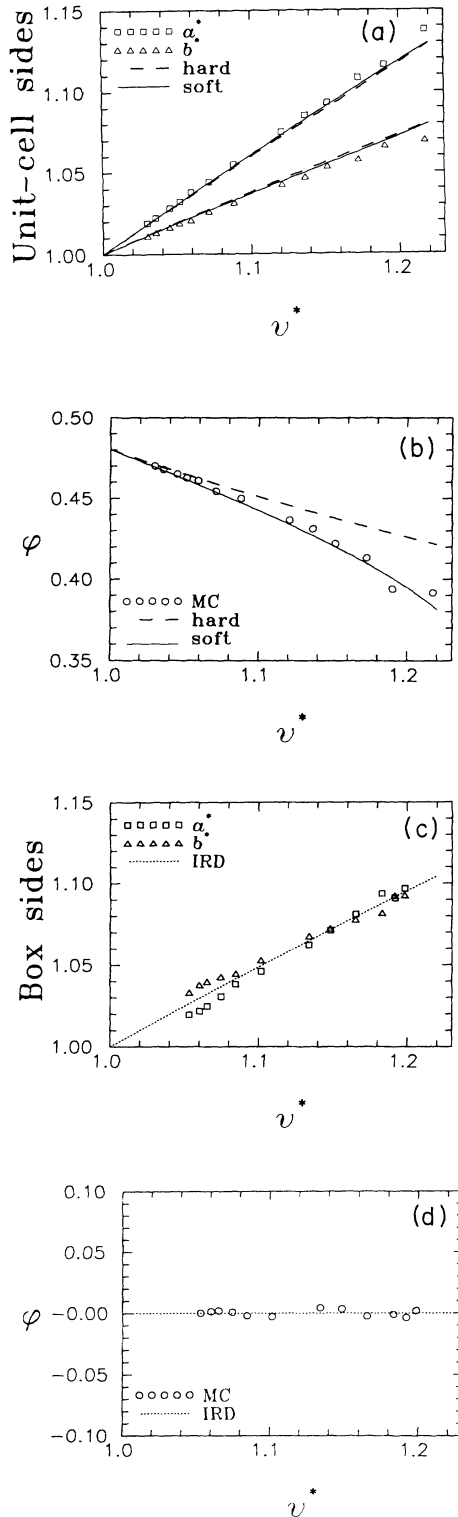


FIG. 7. (a) The relative unit-cell sides and (b) the (single-sublattice) mean orientation (measured in radians) in the HB crystal as a function of the relative area. The experimental data are compared with the two approximations discussed in the text. (c) The relative box sides, and (d) the mean orientation (decreased by $\pi/6$) in the average maximum (see caption to Table I) in the DC phase. The experimental data are compared with the IRD model.

of the same orientations at close packing. The molecular orientation was defined as the angle between the molecular “short” axis and the x axis; the latter was parallel to the direction of the rows formed by neighboring molecules in the sublattices.) The parameters of the experimental structure are compared with two simple models: (i) a hard static model in which the structure is calculated for an n -inverse power interaction between the centers of the disks forming dumbbells and then the limit $n \rightarrow \infty$ is taken; (ii) a soft static model in which the dumbbells interact by a *site-site* effective potential $u(r) = -\frac{2}{3}k_B T \ln(r/\sigma - 1)$ obtained for the hard-disk system in the self-consistent free-volume approximation.^{42,43} It is assumed that only the disks that are nearest neighbors (which have a common side of their Dirichlet polygons) interact with each other. We observe that the differences between these models and the experimental data do not exceed a few percent in the case of the unit-cell sides. This can be seen as good agreement if we take into account the nonanalytic character of the dumbbells interaction and simplicity of the models. In the case of the molecular orientations, the second model is closer to the MC data.

In Figs. 7(c) and 7(d) analogous plots to those shown in Figs. 7(a) and 7(b) are displayed for the DC structure. The experimental data are compared with the IRD model in which overlaps of dumbbells are allowed (to avoid confusion at high densities), but the decoration rule remains intact. As can be seen, the IRD model well reproduces the MC data below $p = 30$. Some differences between the model and the experiment, concerning the “box sides” above this pressure, can be related to the mentioned trapping of the system into a single structure at this pressure. It is worth noticing that the IRD model implies triangular lattice order of the average positions of the disk atoms forming dumbbells. Hence, the DC phase can be thought

TABLE II. Maximal values of the orientational probability density distribution p_{\max} , and the half width of this distribution in the DC state (for the averaged single maximum, see caption to Table I), and in the HB crystal (for a single sublattice).

p^*	DC		p^*	HB	
	p_{\max}	$(\phi - \bar{\phi})^2$		p_{\max}	$(\phi - \bar{\phi})^2$
50.0*	7.48	0.051	60*	72.3	0.0179
40.0	6.78	0.056	50*	62.9	0.0210
35.0	6.68	0.058	40	49.9	0.0267
30.0	6.01	0.064	35	43.6	0.0308
25.0	5.83	0.068	30	37.4	0.0356
20.0*	5.59	0.075	25	31.2	0.0431
15.0	4.67	0.093	20	25.0	0.0539
13.5	4.10	0.106	15	18.1	0.076
12.0*	3.75	0.118	13.5	15.5	0.088
11.0*	3.46	0.133	12	13.9	0.099
10.5*	3.22	0.139	11	11.9	0.122
10.2*	2.98	0.150	10	10.4	0.146
			9	9.01	0.166

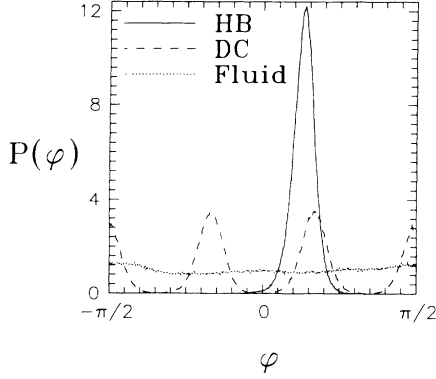


FIG. 8. Typical orientational probability distributions (normalized to π) for the simulated phases. For the HB crystal the distribution for only one of its two sublattices, defined in the text, is plotted. The distribution for the second sublattice is symmetric to the plotted distribution with respect to zero. The curves for the solids correspond to the pressure $p^*=11$, whereas the curve for the fluid to $p^*=8$.

of as an atomic crystal. The structural data for the solids are collected in Table I.

In Fig. 8 typical probability distributions of the molecular orientations are shown for each of the studied phases. The parameters of these orientational distributions for the solid structures are shown in Table II.

IV. FREE-ENERGY CALCULATIONS AND LOCATION OF PHASE TRANSITIONS

The location of the melting transition is approximately known from the hysteresis obtained in the MC simulations by spontaneous freezing of the fluid and spontaneous melting of the solid. For determining the thermodynamic stability of the phases and for locating the expected structural transition in the solid, one needs to know the free energy of the various EOS branches. This allows one to apply Maxwell's double-tangent construction (or an equivalent method) for determining the phase-transition parameters.

In the case of the fluid the free energy (we shall use the *configurational free energy per particle* implicitly every time) can be obtained directly by integrating the pressure excess relative to the ideal gas:

$$f_{\text{fluid}}(v) = f_{\text{id}}(v) + \int_0^p (p - p_{\text{id}}) \rho^{-2} d\rho, \quad (3)$$

$$f_{\text{solid}} = -N^{-1} \ln(Nv^* v_{cp}) + f^{c.m.}(\lambda_{\text{tr}}^{\text{max}}, \lambda_{\text{rot}}^{\text{max}}) - \int_{-1}^1 ds \left[\frac{\partial \lambda_{\text{tr}}}{\partial s} \langle (\Delta_N^2 r)^{c.m.} \rangle_s + \frac{\partial \lambda_{\text{rot}}}{\partial s} \langle (\Delta_N^2 \phi) \rangle_s \right], \quad (7)$$

where $f^{c.m.}(\lambda_{\text{tr}}^{\text{max}}, \lambda_{\text{rot}}^{\text{max}})$ is the free energy of the system with the interaction potential (5), $\langle \dots \rangle_s$ means the thermodynamic average with the interaction potential (5), and s parametrizes λ_j : $\lambda_j(-1)=0$, $\lambda_j(1)=\lambda_j^{\text{max}}$ ($j=\text{tr, rot}$). [The first term on the right-hand side in Eq.

where $f_{\text{id}}(v)/k_B T = -\ln(\pi v) - 1$ is the free energy of the ideal gas of dumbbells. To evaluate the integral on the right-hand side in Eq. (3), we used a sixth-order virial expansion sufficient to fit the fluid data with the exact value of the coefficient B_2 and the coefficient $B_3=0.754B_2^2$ (see Sec. III):

$$p - p_{\text{id}} = B_2 \rho^2 + B_3 \rho^3 + \sum_{k=4}^6 B_k \rho^k. \quad (4)$$

This polynomial was integrated analytically.

In the case of the HB crystal and the DC state, one of the versions of the Einstein crystal method,²⁷ described in Ref. 9, was used after some simple modifications. The method consists in joining the considered solid structure of the system with a harmonic crystal by a thermodynamically reversible path. We used the following interaction potential:

$$U^{c.m.}(\lambda_{\text{tr}}, \lambda_{\text{rot}}) = U_{\text{db}}^{c.m.} + \lambda_{\text{tr}} N (\Delta_N^2 \mathbf{r})^{c.m.} + \lambda_{\text{rot}} N (\Delta_N^2 \phi) = U_{\text{db}}^{c.m.} + U_{\text{EC}}^{c.m.}, \quad (5)$$

where $U_{\text{db}}^{c.m.}$ is the interaction potential of the HHD system (infinity when any two dumbbells overlap, and zero otherwise) with the fixed mass center, and $U_{\text{EC}}^{c.m.}$ will be further referred to as the interaction potential of the Einstein crystal with the fixed center of mass. λ_{tr} , λ_{rot} are some coupling constants varying from zero (in which case the potential corresponds to the pure HHD system with the fixed mass center) to certain maximal values $\lambda_{\text{tr}}^{\text{max}}$, $\lambda_{\text{rot}}^{\text{max}}$ which were chosen so large that the original hard intermolecular interaction gave only a small correction to the free energy of the Einstein crystal. The quantities $(\Delta_N^2 \mathbf{r})^{c.m.}$ and $(\Delta_N^2 \phi)$ are defined as

$$(\Delta_N^2 \mathbf{r})^{c.m.} = N^{-1} \sum_{i=1}^N (\mathbf{r}_i - \mathbf{r}_{0i})^2, \quad (6)$$

$$(\Delta_N^2 \phi) = N^{-1} \sum_{i=1}^N \sin^2(\phi_i - \phi_{0i}).$$

In the above formulas \mathbf{r}_i and ϕ_i ($i=1, 2, \dots, N$) represent the mass center position and orientation of a chosen molecule, respectively, whose reference (lattice) values are \mathbf{r}_{0i} and ϕ_{0i} . The c.m. superscript indicates that a given quantity is related to the system with the fixed center of mass.

The free energy of the HHD system can be evaluated by the following formula:

(7) comes from the moves of the center of mass of the system.] To reduce computational error the s parametrization was chosen in such a way as to make the variation of the integrand with respect to s possibly small; we used the idea of Ref. 27. The integral in Eq. (7) was calculated us-

ing the 10-point Gauss-Legendre method. The values of the averages $\langle \dots \rangle_s$ were obtained by the MC simulations of the system with the interaction potential of Eq. (5). The simulations were performed at the relative area $\nu^* = 1.18$, which is inside the (meta)stability region of both solid phases considered.

The reference values of r_{0i} in the HB crystal corresponded to the unit-cell parameters determined from a power fit in ν^* to the data shown in Fig. 7(a); ϕ_{0i} corresponded to the mean orientations of the dumbbells in the sublattices.

In the DC state the molecular reference positions and orientations (i) were chosen as IRD's of the required density or (ii) were obtained by uniform scaling of the real

close-packed DC structures which were first generated by IRD's and then compressed. In fact, a few molecular arrangements were used to improve the statistics in both cases. The mean free energies obtained using both kinds of reference systems were, within experimental error, essentially the same.

The quantity $f^{c.m.}(\lambda_{tr}^{\max}, \lambda_{rot}^{\max})$, which is the free energy of the system with the interaction potential (5) at $s = 1$, is equal to

$$f^{c.m.}(\lambda_{tr}^{\max}, \lambda_{rot}^{\max}) = f_{EC}^{c.m.}(\lambda_{tr}^{\max}, \lambda_{rot}^{\max}) + f_{corr}, \quad (8)$$

where $f_{EC}^{c.m.}$ is the free energy of an Einstein crystal (with the fixed mass center) which at large λ_j is

$$f_{EC}^{c.m.}(\lambda_{tr}, \lambda_{rot}) = -k_B T N^{-1} \ln [(\pi k_B T / \lambda_{tr})^{N-1} (\pi k_B T / \lambda_{rot})^{N/2} / N], \quad (9)$$

and f_{corr} is the correction to the free energy of the Einstein crystal, coming from the hard-core interactions of the dumbbells:

$$\begin{aligned} f_{corr} &= -k_B T N^{-1} \ln \langle \exp(-U_{db}^{c.m.} / k_B T) \rangle_{EC, s=1} \\ &\equiv -k_B T N^{-1} \ln [P_{system}^{s=1}(\text{no overlaps})]. \end{aligned} \quad (10)$$

The quantity $P_{system}^{s=1}(\text{no overlaps})$ is the probability that no overlap will occur for *noninteracting* dumbbells embedded in the potential $U_{EC}^{c.m.}$. At large λ_j^{\max} , when the multiple overlaps of the dumbbells can be neglected, this probability can be expressed by two-body terms, giving¹²

$$f_{corr} = \frac{1}{2} k_B T P_{single\ db}^{s=1}(\text{overlap}). \quad (11)$$

The probability that a single dumbbell will overlap with another one, $P_{db}^{s=1}(\text{overlap})$, is easy to compute simulating overlaps in the system of noninteracting dumbbells in the field of the EC potential. At large λ_j^{\max} this quantity is very small and even can be neglected if compared to the numerical integration error.

It is worth noticing that from the two different ways of defining the reference configurations in the DC state, the scaled real dense configurations were found to be superior compared to the IRD. This is because the latter required extremely large λ_j^{\max} to reduce the probability of (the multiple) overlaps of the dumbbells. Such overlaps have their source in a very close neighborhood of certain molecular pairs in the IRD; see Fig. 2. Using very large

values of λ_j^{\max} results in increasing computational error.

The values obtained for the free energies of the HB crystal and the DC average structure are collected in Table III. Knowledge of the free energies and the EOS data enable one to calculate the Gibbs free energies:

$$g = f + p\nu. \quad (12)$$

The Gibbs free energies of the solids can be then compared with the Gibbs free energy of the fluid to locate melting. This is shown in Table IV. As it is easy to note, the solid structures have much higher Gibbs free energies than the fluid in the whole hysteresis region. The DC state exhibits, however, the additional degeneracy entropy: $s_{DC} \approx 0.857$ (compare the last column in Table IV). Taking this entropy into account, one locates the melting transition at $p_{melting}^* = 10.5 \pm 0.4$, i.e., within the hysteresis region (see Table V).

The second transition, between the DC state and the HB crystal is located at $p_{DC-HB}^* = 35.7 \pm 0.4$. This pressure is not much different from that at which the system was trapped into a single structure.

V. THE DEGENERACY ENTROPY AND ERGODICITY

As mentioned in Sec. III, without introducing the collective moves the simulated solid structures preserved their molecular arrangements down to melting. On the other hand, the molecular arrangements in the fluid were,

TABLE III. Configurational free energies per particle of the HB crystal and a typical DC structure. The latter is the mean value obtained for a few (seven in each case) reference configurations: (i) obtained by scaling *real* dense structures of the dumbbells and (ii) generated by the IRD's.

Structure	$\lambda_{tr}^{\max} = \lambda_{rot}^{\max}$	Integral	f_{corr}	$f_{EC}^{c.m.} - N^{-1} \times \ln(N\nu^* \nu_{cp})$	f_{solid}
HB	1000	3.904(6)	0.005	8.5869	4.688(6)
DC _{real}	2000	4.663(14)	0.019	9.6205	4.976(15)
DC _{IRD}	50 000	9.486(24)	0.049(4)	14.4201	4.983(28)

TABLE IV. Comparison of the Gibbs free energies for the studied phases in the melting region.

p^*	g_{H-B}	$g_{DC}^{\text{typical struct.}}$	g_{fluid}	g_{DC}
10.2	25.070(7)	25.250(16)	24.374(15)	24.393(16)
11	26.659(7)	26.887(16)	26.030(15)	25.998(16)

of course, varying with “time.” At $p^* = 11.5$ the fluid was observed to freeze spontaneously into a certain non-periodic structure representing the DC phase. These two facts compared with the data collected in Table IV seem to lead to a (double) paradox: (i) The fluid did not freeze into the solid structure of the lowest Gibbs free energy, and, moreover, (ii) it froze into the solid structure whose Gibbs free energy is *higher* than that of the fluid itself. Below we discuss this problem in detail, indicating that such a “paradoxical” behavior can be observed also in simulations of other strongly degenerate systems, e.g., in solid mixtures.

Let us start with the question of whether in the studied model various molecular arrangements corresponding to the DC phase will be preserved when the system size and time of a run tending to infinity. This problem is not only important for melting but plays a crucial role for the structural phase transition in the solid: If there were no transformations from one solid structure to another, this transition would simply not be realizable. The positive answer to the posed question would mean that the various microscopic structures representing the DC phase were different *ergodic components*^{44,45} in the model. In such a case the degeneracy entropy would correspond to *complexity*^{44,45} and, hence, it would not amount to the Gibbs free energy of the model. This would imply, in turn, that the DC phase would not be a thermodynamically stable solid. As it is difficult to imagine any phase of density close to that of the DC phase and, at the same time, with the Gibbs free energy as low as for the DC phase with the degeneracy entropy included,⁴⁶ one would be forced to conclude that the actual melting of the HHD system occurs at much higher pressure⁴⁷ than that at which the spontaneous freezing of the sample of $N = 112$ molecules was observed. However, spontaneous freezing of samples of $N = 448$ and 960 (Ref. 48) dumbbells was observed already at $p^* = 11$ and the frozen structures had densities close to that of the DC phase. A typical structure of the frozen system of $N = 960$ dumbbells at $p^* = 11$ is shown in Fig. 9. As one can see, the centers of mass of atoms (black dots) form a triangular lattice with a few defects. (The atom-atom distribution function of the system was found to be the same as in the case of the defectless system of $N = 112$ dumbbells.) The orientational order of the molecules was analyzed by using the functions

$$g_k(r) = \left\langle \sum_{i < j \leq N} \cos k(\phi_i - \phi_j) \delta(r_{ij} - r) \right\rangle, \quad (13)$$

which are plotted in Fig. 10 for $k = 2, 6$ (ϕ_i, ϕ_j are orientations of two dumbbells whose centers of mass are at the distance r_{ij} and k is an integer). It is clear that the angles between the molecular axes are close to multiples of $\pi/3$ and the angular order is long-range, as expected in the DC phase.

Spontaneous freezing of the large system into the DC phase at $p^* = 11$ strongly suggests that also in the thermodynamic limit the system will freeze near $p = 11$ into the same phase. This, however, requires including the degeneracy entropy into the Gibbs free energy of the solid. In other words the distinct molecular arrangements cannot be preserved in the DC phase, which has to be ergodic. Obviously, ergodicity cannot be proved by computer simulations. However, simulations can provide some supporting arguments. Such an argument concerning ergodicity of the DC phase is described below.

Different solid structures are represented by small regions of the configurational space, which at close packing “shrink” to single points or zero-volume sets. To characterize the time evolution of the system one can use, for example, the quantities $(\Delta_N^2 \mathbf{r})^{\text{c.m.}}$ and $(\Delta_N^2 \phi)$, see Eq. (6), where the reference configuration corresponds to an initial structure. In Fig. 11 the time dependence of the above quantities, characterizing the “penetration” of the configurational space by a point representing the system, is presented at two densities. The lower density was chosen in the melting transition region, whereas the higher density corresponds to the stable solid. These runs, much longer than those used to calculate the EOS,

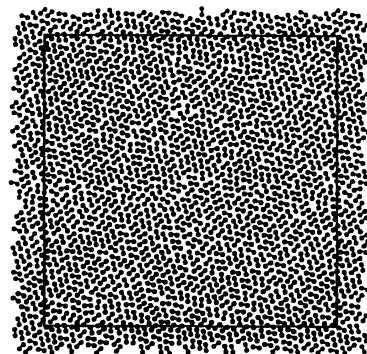


FIG. 9. Typical configuration of $N = 960$ dumbbells frozen into a solid at $p^* = 11$. Centers of disks forming dumbbells (black dots) are connected by line segments. The periodic box is marked by a continuous line.

TABLE V. Pressures and densities of the phase transitions.

Transition	p^*	ρ_{lower}^*	ρ_{upper}^*
Melting	10.5(4)	0.812(5)	0.839(6)
Structural	35.7(4)	0.9388(6)	0.9521(7)

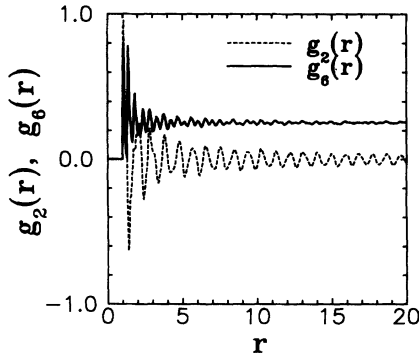


FIG. 10. Orientational corrections of $N=960$ dumbbells at $p^*=11$.

were performed in the NVT ensemble, which is computationally cheaper for these quantities than the NpT ensemble. In both cases the initial configurations were the IRD's of the required density. It is worth noting here that because the distances in the configurational space between the neighboring points representing centers of the regions (corresponding to different solid structures) are of order unity, the change of $(\Delta_N^2 r)^{c.m.}$ by $\approx 1/N$ can be interpreted as "visiting" a new structure by the system [the analogous is true for $(\Delta_N^2 \phi)$ at the beginning of the "walk"; this quantity should saturate at 0.5]. As can be seen in Fig. 11(a), at the lower density the system

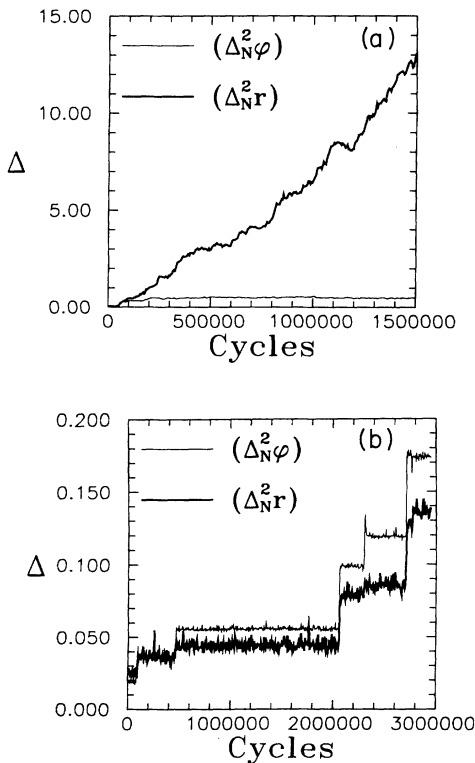


FIG. 11. Time dependence of the diffusional parameters $(\Delta_N^2 r)^{c.m.}$ and $(\Delta_N^2 \phi)$ (a) in the transition region ($v^*=1.22$), and (b) for a randomly chosen structure of the DC phase ($v^*=1.19$).

"wanders" through many structures, whereas at the higher density it remains trapped into certain structures for a very long time. A few "steps" shown in Fig. 11(b) indicate, however, that some rearrangements of the molecular structures (which were independently monitored by direct observations of the structure of the system) have occurred in the system. Frequency of such rearrangements is, however, by a few (at least three) orders of magnitude lower than in the coexistence region (or in the fluid, where it is even higher). Nevertheless, their presence provides an argument for the existence of nonzero-measure connections in the configurational space between the different solid structures⁴⁹ and, hence, ergodicity of the solid. As easy to note, the mean "times" between the consecutive transformations much exceed the lengths of the runs used for the evaluation of the EOS. This is one of the reasons why the HB structure remained unchanged down to melting in spite of much higher Gibbs free energy than in the DC phase.⁵⁰

Although the above discussion indicates that the DC phase is ergodic, the observed time behavior of the fluid at freezing still requires a comment. The lifetime of various defectless DC arrangements near melting are about ten times larger than the length of a single run. On the other hand, the freezing of the (ergodic) fluid occurs in a single run. Hence, taking into account considerations described in Ref. 48 one could ask why the sample freezes when in the solid state the degeneracy entropy is practically not available to it within a single run. The answer to this question can be obtained if one considers defects (vacancies and dislocations) contained in the structures into which the fluid freezes. The defects "speed up" transformations between various DC structures. The example illustrating this fact is given in Fig. 12, where a plot analogous to those shown of Fig. 11 is shown for $N=111$ dumbbells (and a monomolecular vacancy). Thus, the defects, which have to be created spontaneously in large systems, can be thought of as a mechanism stabilizing the DC phase. (They should also play an important role in the dynamics of the phase transitions between this phase and other phases.)

It is worth adding that a spontaneous creation of the defects in an initially defectless DC structure requires

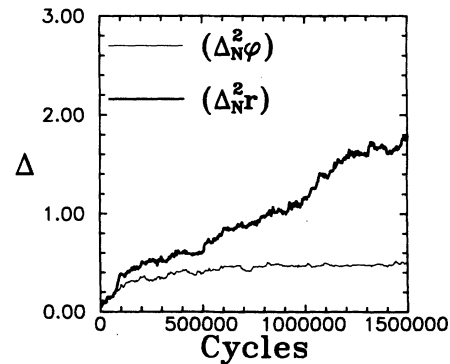


FIG. 12. Same as in Fig. 11 for $N=111$ dumbbells with a vacancy in the DC phase at $v^*=1.179375$, i.e., at the same number density as in Fig. 11(b).

much larger samples than that studied here. A system of $N = 1008$ dumbbells at $p^* = 11$, obtained from nine replicas of a defectless sample of $N = 112$ dumbbells, remained defectless within 10^5 cycles, and no self-diffusion of the molecules was observed in it.

A few runs were also performed in the NpT ensemble for a 1:1 mixture of two kinds of hard disks of infinitesimally small difference of radii. In the latter system the mixing entropy plays a similar role to the degeneracy entropy in the HHD system. Three sizes of the system were simulated at the relative area $\nu^* = 1.2544$; the length of each run was 10^6 cycles. Only in the largest system was a spontaneous creation of defects observed (after about 3×10^4 cycles). The dependence of $(\Delta_{Nr}^2)^{c.m.}$ on the cycle number was similar to that of Fig. 11(a). In the smaller systems defects were not created, and the time evolution of $(\Delta_{Nr}^2)^{c.m.}$ was similar to that shown in Fig. 11(b).

We will now discuss the influence of the defects on the EOS. The structures used to generate the EOS in the solid were defectless, and it is not known *a priori* whether and how defects will modify the data in Table I. The influence of the defects on the EOS and the transition location can be estimated from the density difference between the DC structure into which the fluid of $N = 960$ dumbbells froze spontaneously and that simulated for $N = 112$. At $p = 11$ this difference is less than $\Delta\rho^* = 0.002$,⁴⁸ i.e., does not exceed the error of a single run. It is easy to check that such a difference has negligible influence on the location of melting. In the case of the structural transition in the solid the matter is not as obvious. (Computing the Gibbs free energy of the DC phase near the structural transition to the HB crystal one integrates the EOS on a much larger interval than in the case of melting.) Even in that case, however, we do not expect any substantial corrections because any systematic decrease of the density of the DC phase coming from defects will likely be accompanied by a similar decrease of the density of the HB crystal (coming from the same reason). Hence, the transition pressure will likely remain unchanged, within the estimated error. At the high densities at which this transition occurs the density of defects should be much smaller than at melting, and, hence, the estimated errors for the transition densities should be also valid.

VI. SUMMARY

Using the MC simulations for the system of hard dumbbells of the anisotropy parameter $d^* = 0.924$, we have shown the existence of two phase transitions in the system: the first, between the fluid and the aperiodic DC phase, and the second, between the DC phase and a high-density solid, represented in this work by the HB crystal. The equation of state, the structural properties of the phases, and their free energies were determined. The phase transitions were located.

We do not claim that the high-density phase of the system is actually the HB crystal.⁵¹ However, taking into

account the fact that various crystalline structures recently studied in the hard dimer system¹⁹ exhibit, within experimental error, the same isotherms and the same free energies, which are lower than the free energies of single aperiodic solid structures, we expect that the same will hold for the structures of the dumbbells studied here. Hence, assuming that the close-packed structure of the dumbbells ($d^* < 1$) on the plane has a degeneracy entropy equal to zero, we expect that (i) the structure of the high-density phase is crystalline and (ii) the determined transition densities between the DC phase and the HB crystal are, within the experimental accuracy of the present work, correct for this phase. Comparing the results obtained in this paper with the results of Ref. 19, one can expect that the DC phase is stable down to $d^* \approx 0.8$, i.e., in a rather broad range of the anisotropy parameter.

The structural transformation in the solid is an example of a phase transition in a continuous homomolecular system in which (at least) one of the coexisting solid phases is aperiodic with respect to the positions of the molecular centers of mass. It has been explicitly shown that the degeneracy entropy of the DC phase, being a global property of this thermodynamic state, is responsible for the thermodynamic stability of this phase. It is worth stressing that at the time and size scales of the simulations performed this entropy is frozen in the defectless solid phases, and “activates” only in the presence of defects. The latter, which have to be created spontaneously in large samples, are expected to play a significant role in the stabilizing of the DC phase.

Finally, it is worth noting that calculations described above are in qualitative agreement with the free-volume approximation described in Ref. 20. This approximation predicts a phase transition from the high-density phase to the DC phase when d^* is increased from a certain (less than one) value at which the first phase is stable. The aperiodic molecular DC phase can be thought of as an atomic crystal of the disk atoms forming dumbbells. At the same time, the high-density crystalline phase can be considered as an example of a molecular crystal. In certain systems of real diatomic molecules a phase transition between molecular and atomic crystal was observed at very high pressure.⁵² If we assume that the increase of pressure results in decreasing the effective atomic radii without any (or with smaller) decrease of the intramolecular bond length (as it occurs in J_2 ;⁵² in such a case d^* increases), then the HHD system can be thought of as the simplest model reproducing such a transition in 2D.

ACKNOWLEDGMENTS

The author would like to thank Professor Daan Frenkel for his interest in this work, helpful discussions, and correspondence; Dr. Piotr Pierański, for encouragement; and Professor E. Tosatti, for critical comments. He is also grateful to Professor M. P. Tosi for making it possible for the author to work at the International Centre for Theoretical Physics (ICTP), and to Professor Abdus

Salam, the International Atomic Energy Agency and UNESCO for hospitality at the ICTP. Thanks are also due to Dr. A. Nobile for help during these computations, to Dr. E. Canessa and Dr. V. Kumar for useful remarks, and to Dr. J. Veerman for a helpful suggestion concerning the simulations.

APPENDIX A: ON THE ENTROPY OF HARD DUMBBELLS AT CLOSE PACKING

Figure 4 in the text shows that the close-packed structures of the dumbbells can be mapped onto a certain lattice model. The lattice model consists of a triangular lattice decorated by trimers: (i) Each lattice site is occupied by a center of one trimer and two ends of other trimers and (ii) some configurations of trimers are excluded. The configurations excluded are the so-called K configurations in which centers of the trimers with ends occupying a chosen lattice site are located on the same side of the line defined by a trimer whose center occupies this site. In order to eliminate "parallel" analogs of the K configurations, it is convenient to represent certain trimers by tilde marks (or their mirror images).

The lattice model defined is useful for classifying various close-packed structures of the dumbbells and for estimating the entropy per particle of the close-packed structure of the dumbbells in the thermodynamic limit. Estimating this entropy, one should neglect the difference between a tilde and its mirror image. This is because replacing the tilde by its mirror image in a part of the lattice (if such a replacement is allowed by the decoration rules, i.e., if it does not lead to the K configurations), one gets new configurations of the dumbbells only for infinitely long lines of parallel trimers. It is easy to show that the contribution to the entropy per trimer, coming from such configurations, is zero in the thermodynamic limit. (The same is obviously true for replacing all trimers by their mirror images.) It is easy to prove that the necessary condition for a positive value of the entropy per particle in the model is the existence of some *finite* clusters, which could be changed with no influence on the remaining part of the lattice. (Otherwise the number of states in the system can be bounded by the number of states of the boundary of the system, which immediately leads to the zero entropy per particle in the thermodynamic limit.) We have not found such clusters and hence, we expect that the entropy per trimer is zero. This implies that the degeneracy entropy per dumbbell at close packing should be zero in the thermodynamic limit.

It is worth noting that for a lattice model analogous to that described above, but defined on a square lattice, one can immediately show that the entropy per particle is zero in the thermodynamic limit. This follows from the fact that the number of different decorations of a finite

$M \times M$ square lattice is less than 2^{2M} . This number is a crude upper limit for the number of decorations of two neighboring rows, each of M sites; the decoration of the remaining rows is then uniquely determined. The entropy per particle is then less than $2M^{-1} \ln 2$.

APPENDIX B: CLUSTER MOVES

The trial cooperative moves were performed in sequences consisting of N trial moves of individual clusters. Each of the latter moves can be divided into four parts.

(1) One of the dumbbells is randomly chosen. (The same dumbbell can be chosen a few times in a single sequence of N moves.)

(2) The kind of the cluster we attempt to move is tossed. (The probability of tossing any of the three kinds of clusters, see Fig. 5, should be positive, but its value is arbitrary. It was found that the acceptance ratio for small clusters is higher than for large ones, decreasing roughly by one order of magnitude if the cluster is enlarged by one molecule. Moreover, moves of smaller clusters require less computer time. Hence, to increase efficiency of the structure evolution, the probability of choosing a pair cluster was taken 0.9 and the remaining two probabilities were equal 0.05.)

(3) The clusters of the tossed kind (shape) that contain the chosen dumbbell are searched for. Let $i(c)$ be the number of such clusters and $i_{\max}(c)$ be the upper limit for $i(c)$ (c represents the kind of cluster: $c=2, 3, 4$ for a pair, a triplet, and a quadruplet, respectively). It is easy to check that in any IRD packing $i_{\max}(2)=i_{\max}(3)=2$ and $i_{\max}(4)=4$. These numbers were also found to be maximal in simulations of the DC solid with an operational definition of the clusters used in the simulations.

(4) If the number of the clusters searched for in part 3 is positive [$i(c) > 0$] then a random number, $0 \leq \xi < 1$, is generated, and if $\xi < i(c)/i_{\max}$ one of these clusters (randomly chosen) is replaced by its mirror image with respect to an axis containing the mass center of the chosen cluster and a rescaled position of a center of one of its atoms, chosen randomly (for quadruplets only the four atoms closest to the cluster mass center are considered). The rescaling was applied because the acceptance ratio for the cluster moves was found to increase slightly if in place of the real positions of atoms, \mathbf{r} , rescaled positions, \mathbf{r}' , were used according to the formula

$$\mathbf{r}' - \mathbf{r}_c = \alpha(\mathbf{r} - \mathbf{r}_c),$$

where \mathbf{r}_c is the mass center of the dumbbell to which the considered atom belongs, and $\alpha \approx \sqrt{v^*/d^*}$ is a constant within a single run.

If no overlap is found after the replacement in 4⁰, the whole move is accepted. Otherwise the previous configuration is not changed.

One can check that the cluster moves fulfill microscopic reversibility.

*Permanent address.

- ¹B. J. Alder and T. E. Wainwright, *J. Chem. Phys.* **33**, 1439 (1960).
- ²J. Vieillard-Baron, *J. Chem. Phys.* **56**, 4729 (1972); see also J. Cuesta and D. Frenkel, *Phys. Rev. A* **42**, 2126 (1990).
- ³A. C. Brańka, P. Pierański, and K. W. Wojciechowski, *J. Chem. Phys. Solids* **43**, 817 (1982); see also K. W. Wojciechowski, A. C. Brańka, and M. Parrinello, *Mol. Phys.* **53**, 1541 (1984).
- ⁴D. Bernal, *Proc. R. Soc. London, Ser. A* **280**, 299 (1964); J. L. Finney, in *Amorphous Solids and the Liquid State*, edited by N. H. March and M. P. Tosi (Plenum, New York, 1985).
- ⁵B. J. Ackerson, *J. Phys. Condens. Matter* **2**, SA389 (1990).
- ⁶W. Kranendonk and D. Frenkel, *J. Phys. Condens. Matter* **1**, 7735 (1989).
- ⁷W. G. Hoover and F. H. Ree, *J. Chem. Phys.* **49**, 3609 (1968).
- ⁸R. Eppenga and D. Frenkel, *Mol. Phys.* **52**, 1303 (1984).
- ⁹D. Frenkel and B. Mulder, *Mol. Phys.* **55**, 1171 (1985).
- ¹⁰A. Stroobants, N. H. W. Lekkerkerker, and D. Frenkel, *Phys. Rev. A* **36**, 2929 (1987).
- ¹¹D. Frenkel, *Liq. Crystals* **5**, 929 (1989).
- ¹²J. A. C. Veerman and D. Frenkel, *Phys. Rev. A* **41**, 3237 (1990).
- ¹³B. J. Alder and T. E. Wainwright, *Phys. Rev.* **127**, 359 (1962).
- ¹⁴C. Carlier and H. L. Frisch, *Phys. Rev. A* **6**, 1153 (1972); F. H. Ree and T. Ree, *J. Chem. Phys.* **56**, 5434 (1972).
- ¹⁵A. C. Brańka and K. W. Wojciechowski, *Phys. Rev. Lett.* **50**, 846 (1983).
- ¹⁶A. C. Brańka and K. W. Wojciechowski, *Phys. Lett.* **101A**, 349 (1984); see also *Mol. Phys.* **72**, 941 (1991).
- ¹⁷D. Frenkel and R. Eppenga, *Phys. Rev. A* **31**, 1776 (1985).
- ¹⁸A. C. Brańka and K. W. Wojciechowski, *Mol. Phys.* **56**, 1419 (1985).
- ¹⁹K. W. Wojciechowski, D. Frenkel, and A. C. Brańka, *Phys. Rev. Lett.* **66**, 3168 (1991); K. W. Wojciechowski, A. C. Brańka, and D. Frenkel (unpublished).
- ²⁰K. W. Wojciechowski, *Phys. Lett. A* **122**, 377 (1987).
- ²¹As nonconvex bodies are qualitatively different from convex ones, one can expect qualitatively different behaviors in certain situations. An example is a simple model with a negative value of the Poisson's ratio: K. W. Wojciechowski and A. C. Brańka, *Phys. Rev. A* **40**, 7222 (1989). It is worth adding that "unit cells" of real materials with a negative Poisson's ratio are also nonconvex: R. Lakes, *Science* **235**, 1038 (1987).
- ²²Y. T. Cheng and W. L. Johnson, *Science* **235**, 997 (1987).
- ²³For a review see K. Binder and A. P. Young, *Rev. Mod. Phys.* **58**, 801 (1986); I. Ya. Korenblit and E. F. Shender, *Usp. Fiz. Nauk* **157**, 267 (1989) [*Sov. Phys. Usp.* **32**, 139 (1989)].
- ²⁴For reviews on quasicrystals see, e.g., *The Physics of Quasicrystals*, edited by P. J. Steinhardt and S. Ostlund (World Scientific, Singapore, 1988); *Quasicrystals the State of the Art*, edited by D. P. DiVincenzo and P. J. Steinhardt (World Scientific, Singapore, 1991). In certain materials, sharpening of the quasicrystalline diffractive peaks was observed when the temperature was increased: P. Bancel, *Phys. Rev. Lett.* **63**, 2741 (1989). These are the so-called entropic quasicrystals; see Ref. 25.
- ²⁵M. Widom, K. J. Strandburg, and R. H. Swendsen, *Phys. Rev. Lett.* **58**, 707 (1987); C. L. Henley, *J. Phys. A* **21**, 1649 (1988); M. Widom, D. P. Deng, and C. L. Henley, *Phys. Rev. Lett.* **63**, 310 (1989); K. J. Strandburg, L.-H. Tang, and M. V. Jarić, *ibid.* **63**, 314 (1989).
- ²⁶K. W. Wojciechowski (unpublished).
- ²⁷D. Frenkel and A. J. C. Ladd, *J. Chem. Phys.* **81**, 3188 (1984).
- ²⁸See, e.g., R. D. Diehl, C. G. Shaw, S. C. Fain, and M. F. Toney, in *Ordering in Two Dimensions*, edited by S. K. Sinha (North-Holland, New York, 1980).
- ²⁹R. H. Fowler and G. S. Rushbrooke, *Trans. Faraday Soc.* **33**, 1272 (1937). For better estimates of the degeneracy entropy, see J. F. Nagle, *Phys. Rev.* **152**, 190 (1966); see also A. J. Phares and F. J. Wunderlich, *J. Math. Phys.* **27**, 1099 (1986).
- ³⁰At certain $d^* \neq 1$ one can construct clusters which are *locally* denser than the HB crystal at close packing. [It is particularly easy to construct an example at $d^* = 1/\sin(\pi/12)$.] However, such clusters do not fill the space, and structures containing them are believed to be *globally* less dense than the HB crystal.
- ³¹The oblique lattice, shown in Fig. 1(c), contains only one molecule per unit cell and, in principle, is the simplest crystalline structure of the dumbbells. The specification of its unit cell, however, requires one more parameter (e.g., the angle between the unit-cell sides) than in the case of the HB crystal (which has a rectangular lattice). As this might reduce the accuracy of the free-energy determination, the HB crystal was used to exemplify the highest-density state of the system.
- ³²N. D. Mermin, *Phys. Rev.* **176**, 250 (1968).
- ³³W. W. Wood, in *Physics of Simple Liquids*, edited by H. N. V. Temperley, J. S. Rowlinson, and G. S. Rushbrooke (North-Holland, Amsterdam, 1968).
- ³⁴R. Najafabadi and S. Yip, *Scr. Metall.* **17**, 1199 (1983).
- ³⁵S. Yashonath and C. N. R. Rao, *Mol. Phys.* **54**, 245 (1985).
- ³⁶To avoid rotation of the system, the direction of one of the box sides was kept parallel to the x axis of the laboratory coordinate frame.
- ³⁷This is easy to show if one tries to construct any IRD without such clusters.
- ³⁸T. Boublik, *Mol. Phys.* **63**, 685 (1988).
- ³⁹B. Barbooy and W. M. Gelbart, *J. Chem. Phys.* **71**, 3053 (1979).
- ⁴⁰J. Talbot and D. J. Tildesley, *J. Chem. Phys.* **83**, 6419 (1985).
- ⁴¹J. S. Rowlinson, J. Talbot, and D. J. Tildesley, *Mol. Phys.* **54**, 1065 (1985).
- ⁴²J. G. Kirkwood, *J. Chem. Phys.* **18**, 380 (1950).
- ⁴³W. W. Wood, *J. Chem. Phys.* **20**, 133 (1952).
- ⁴⁴R. G. Palmer, *Adv. Phys.* **31**, 699 (1982).
- ⁴⁵C. D. van Enter and J. L. van Hemmen, *Phys. Rev. A* **29**, 355 (1984).
- ⁴⁶One could speculate about a kind of a plastic crystal because releasing of the orientational degrees of freedom can offer the entropy per molecule comparable to s_{deg} . No such hypothetical phase was, however, observed in the simulations.
- ⁴⁷For example, freezing into the HB crystal, which is more stable than a typical structure of the DC phase (see Table IV) and, probably, the most stable periodic crystal, would occur about $p^* = 22$. (This value of the pressure was obtained assuming linear dependence of $\Delta g = g_{\text{HB}} - g_{\text{fluid}}$ on p^* .)
- ⁴⁸The system of $N = 960$ dumbbells was equilibrated in a square box at $p^* = 5.5$. In subsequent runs (each of 2×10^4 cycles) the pressure was increased by $\Delta p = 1$ up to $p = 10.5$. At $p^* = 9.5$ the density of the system was computed in an extra run of the same lengths, giving $\rho = 0.797$, which is in good agreement with the density obtained for $N = 112$. At $p^* = 10.5$ two longer (5×10^4 cycles) runs were performed with the box allowed to choose any rectangular shape. Large fluctuations were observed in both runs. In the first of these runs a drift of the density toward higher values was observed (the average density was by about 0.005 larger than at

$N=112$), suggesting beginning of freezing of the system. The system did not freeze, however, in the second run, in which the density had decreased by 0.003. In the next run (of 2×10^5 cycles) the pressure was increased to $p^* = 11$, and the system froze into a defected DC structure of $\rho^* = 0.843$.

⁴⁹In the case of large systems the “diffusion” in the configurational space should be supported by various defects which are expected to be spontaneously created in the solid.

⁵⁰The additional reason is the structural difference between the HB and DC phase, which “disfavors” molecular rearrangements in the defectless HB crystal.

⁵¹In fact, the HB solid was used only as a simple and computationally convenient example of the close-packed structure of the dumbbells. See also Ref. 31.

⁵²K. Takemura *et al.*, Phys. Rev. B **26**, 998 (1982).